Numerical Simulation of Detonation in a Valveless Pulsed Detonation Chamber

Ionut Porumbel
Romanian Research and Development Institute for Gas Turbines COMOTI
Scientific researcher
220D, Iuliu Maniu Blvd., Bucharest*, sector 6, 061126, Romania*
ionut.porumbel@comoti.ro

Bogdan G. Gherman
Romanian Research and Development Institute for Gas Turbines COMOTI
Head of Computational Fluid Dynamics Department

Ion Malael
Romanian Research and Development Institute for Gas Turbines COMOTI
Scientific researcher

Valeriu Dragan
Royal Institute of Technology
Post doctoral researcher
Brinellvägen 8, 114 28, Stockholm, Sweden

ABSTRACT

The paper presents Reynolds Averaged Navier Stokes numerical simulation of the premixed, detonation flow inside a valveless pulsed detonation chamber. The control of the admission of the fresh mixture is achieved through a shock wave system generated by the interaction of two supersonic jets impinging on a Hartmann oscillator. Several phases in the operation of the detonation chamber can be observed in the numerical simulation. The numerical simulation shows that self – ignition of the fuel – air mixture occurs at 0.150 ms after the flow starts to flow into the PDC, in two symmetrical positions inside the lateral resonators, in the straight channel at the middle of their vertical dimension and around the middle of the straight channels of the resonators, in the axial direction. After this, during the propagation phase, the temperature inside the supersonic nozzle remains high enough to continue to ignite the fresh mixture whenever the pressure in the divergent section of the nozzle is low enough to allow it to enter the computational domain. Once the inlets close, the temperature starts decreasing throughout the combustor, with high temperature regions being maintained towards the outlet, where the influence of the hot central jet core is still present, and near the PDC walls. The lateral resonators cool much faster, since their temperature was much lower at the beginning of the cycle. The numerical data is analyzed, and the shortcomings of the numerical simulation are discussed. Future solution for improving detonation modeling are proposed.

KEYWORDS: *RANS, detonation, supersonic combustion*

1 INTRODUCTION

Pulsed detonation chambers (PDC) are not a novel research issue. The detonation and deflagration processes have been studied intensely in the last century. The detonation process was observed for the first time in gaseous fuels by Bertolet in 1881. Later on, Chapman [1] and Jouguet [2] discovered that the products resulted from the detonation propagate at sonic speed relative to the detonation wave. The studies showed a fast energy convergence rate that occurs during detonation, corroborated to much higher thermodynamic efficiencies compared to the deflagration process.

While remaining an exotic phenomenon, of strictly academic interest, for quite a while, the study of detonation took an important step forward in the interest of combustion researchers in the mid-XX century, as supersonic flight appeared as an achievable possibility. A first approach was the definition

of various thermodynamic cycles aiming at modelling the detonation powered engine, improving on the Chapman - Jouguet theory. A first attempt was the development of the Humphrey cycle [3], based on constant volume heat addition with an isentropic expansion and an isobaric heat rejection. Another cycle used for shocks and detonation wave engines is the ZND (Zeldovich–von Neumann–Doring) cycle [4]. The theory defines an intermediate state, the ZND point, defining the chemical reaction start point. Another cycle worth mentioning is the Fickett-Jacobs cycle [5].
Over the last decade, the application of the above mentioned cycles was studied in several analyses (e.g. [6] performed with various degrees of success. A detailed review of the work carried out in the field of PDC design, including theoretical and experimental approaches, can be found in [7].
The application of detonation waves in propulsion system dates back to the 1940s [8], but the complexity of the problem delayed the first successful demonstrator flight to as late as 2008 (DARPA's Blackswift [9]). The demonstration flight was, however, at low speed, and the project was soon cancelled. During this time, a significant number of PDC constructive solutions has been proposed, none completely successful: pure (e.g. [10] combined-cycle (e.g. [11]) and hybrid (e.g. [12]). The pure PDC is comprised of one or more detonation tubes an inlet and a nozzle. The main problem of the solution is the low inlet pressure at high altitudes. The combined-cycle PDC is typically used for ramjets or scram jets. However this type of engine only works efficiently until Mach 5 [13]. The hybrid PDC replaces the classical deflagration combustor with a PDC to enhance the engine performance, reduce flight time and, possibly, decrease pollutant emission.
The optimal PDC operating frequency has been an important research objective. To approach the performances of a classical gas turbine engine, the PDC must operate at least at 75 Hz for a near stoechiometric fuel air mixture [14]. Increasing the frequency allows for a reduction in the combustor size, and engine weight and drag. One solution [15] for high frequencies proposes a series of out-of-phase initiation chambers connected to a main PDC. Another frequency increasing solution, applicable for mechanical valves, is to reduce the deflagration phase time by enhancing the fuel-air mixing, either through increasing the turbulence [16], or through controlling the geometry [17].
Aerodynamic valve solutions have also been used in some PDC applications. The most important requirement related to this approach is to prevent the flashback. Proposed solutions were to place a detonation initiator equipped with an aerodynamic isolator at the chamber inlet [18], or to accelerate the flow to the supersonic regime upstream of the combustor inlet [19]. Other valveless high frequency solutions (e.g. [20]) propose the generation of high frequency oscillations at the combustor inlet, though the interaction of supersonic jets, or by using stationary or moving walls. A wedge-shaped object detonation wave stabilization concept [21] initiates the detonation wave through the coupling of the reaction waves with the leading shock waves. The solutions present several important advantages related to better mixing, ease of initiation, flashback prevention, detonation control, reduced size, low emissions and stability [22]. Rotating, tangential exhaust PDCs has also been recently proposed (e.g. [23]), based on a quite old pioneering idea [24], but operating at low frequency and inlet pressure. An extensive review of the current state-of the art can be found in [25].
The paper presents Reynolds Averaged Navier Stokes (RANS) numerical simulation of the premixed, detonation flow inside a valveless PDC, which is part of a novel detonation engine [26]. The control of the admission of the fresh mixture is achieved through a shock wave system generated by the interaction of two supersonic jets impinging on a Hartmann oscillator [27].

2 SIMULATION SETUP

The geometry of the PDC used for the numerical simulation is presented in Fig. 1. To diminish the computational load, the computational domain presented in Fig. 2 was simplified by removing the subsonic part upstream of the critical section of the Laval nozzles and was discretized by a three dimensional computational grid, to a total of 2,180,546 computational cells, on a structured, Cartesian grid, shown in Fig. 1. The cell size varied between 0.1 mm and 0.52 mm, with the smaller values near the walls. The estimated Kolmogorov scale is of 1.6 μm, placing the resolution within RANS scope.
The boundary conditions imposed on the computational domain were of the following types:

- Solid, no-slip, adiabatic wall boundary conditions;
- Sonic inflow boundary conditions ($p^* = 6$ bar, $T^* = 500$ K; $M = 1$, Gas composition: Hydrogen / air stoechiometric mixture);
- Extrapolation supersonic outflow.

The numerical simulation used the ANSFYS CFX commercial solver, using the pressure based with the SIMPLE (semi-implicit methods for pressure linked equations) numerical method. The turbulence model was the k - ε model [28], widely used in combustion research, with reasonable results for high Reynolds number cases [29]. Finite rate chemistry described by a one – step simplified reaction mechanism [30] and the EDM combustion model [31], was used to describe the chemistry. The model was selected as the best CFX available compromise between computational load and accuracy.

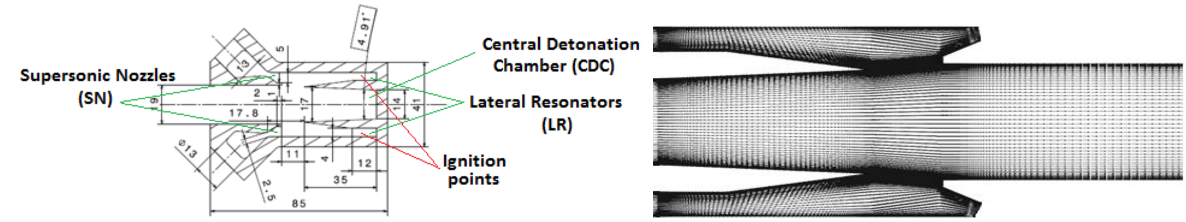

Figure 1 – Computational domain (left) and discretization grid (right)

3 RESULTS AND DISCUSSION

The numerical simulation allowed the observation of four phases in the operation of the studied PDC: the ignition phase, the propagation phase, and cooling phase, and the readmission phase.

3.1 The ignition phase: 0.000 - 0.250 ms

The first important aspect that was verified through the reactive flow numerical simulation was the self ignition of the fuel / air mixture and the initiation of the detonation wave inside the PDC. Fig. 2 presents the temporal evolution of the flow temperature between 0 ms and 0.25 ms.
The numerical simulation shows that self – ignition of the stoechiometric fuel – air mixture occurs at 0.150 ms after the flow starts into the PDC, in two symmetrical positions in the LR, shown in Fig. 1.

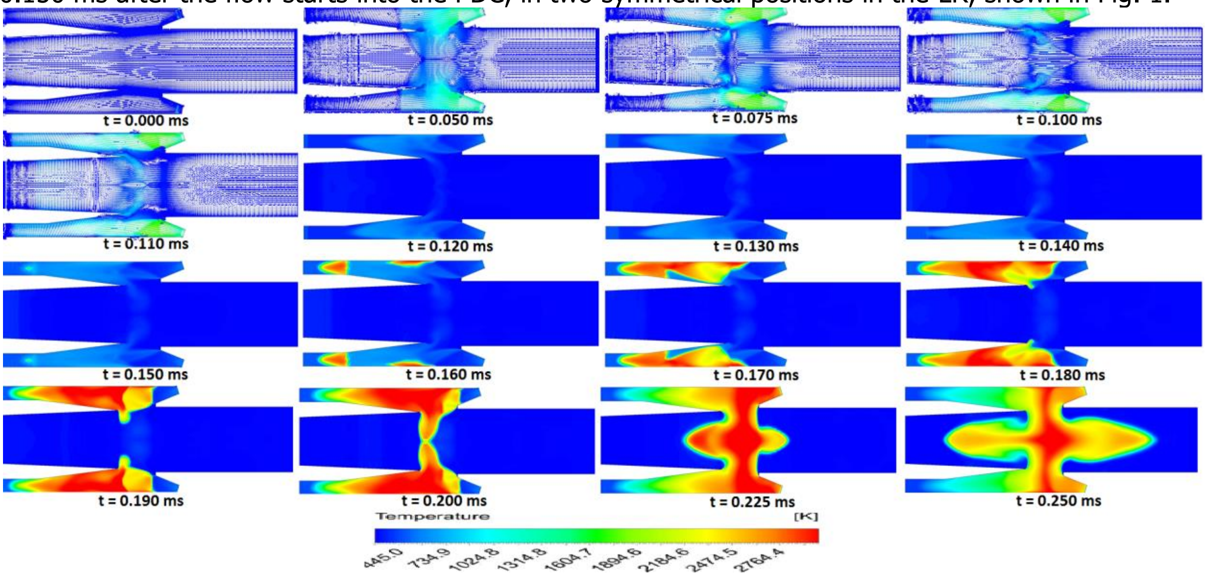

Figure 2 – Temperature scalar field evolution during the ignition phase

To better understand the flow through the PDC, the temporal evolution of the velocity vector field, and the scalar fields of pressure, and Hydrogen and water mass fractions are presented in Figs. 3 - 6.
The flow enters the PDC with a slightly higher temperature (500 K) than the atmospheric air, visible in light blue in Fig. 2. A bow expansion wave appears at the SN exit. The air streams issuing from the two SN first enter the two LR (Fig. 3), where they create pressure waves propagating axially along the flow direction both in the LR, and into the CDC (Fig. 4). As the Supersonic Jets (SJ) flow into the LR, the flow is entrained from the stagnant CDC into the LR (Fig. 3), increasing the pressure levels there, and the intensity of the pressure waves propagating inside the LR. The entrained air interferes with the incoming jets composed of premixed Hydrogen and air and creates, around t = 0.050 ms, vortices that pushed the combustible mixture into the CDC (Fig. 5).
The mixture in this region is then slowly convected in both axial and transversal directions by the low velocity flow existing here, and will play a critical role in the transition from deflagration to

detonation. The pressure waves mentioned earlier reach the back wall of the LR between t = 0.110 - 120 ms (Fig. 4), and the pressure near the closed ends of the LR starts raising sharply. The pressure waves are reflected back by the back wall of the LR and start moving towards the incoming SJ (Fig. 4), which are still flowing towards the LR closed ends (Fig. 3). The flow behind the pressure waves reverses direction entrained by the pressure gradient. When the pressure waves returning from the back wall meet the incoming jets, the local pressure increases even higher and forces the flow in the SJ to break suddenly, triggering the formation of a shock wave around the middle of the LR.

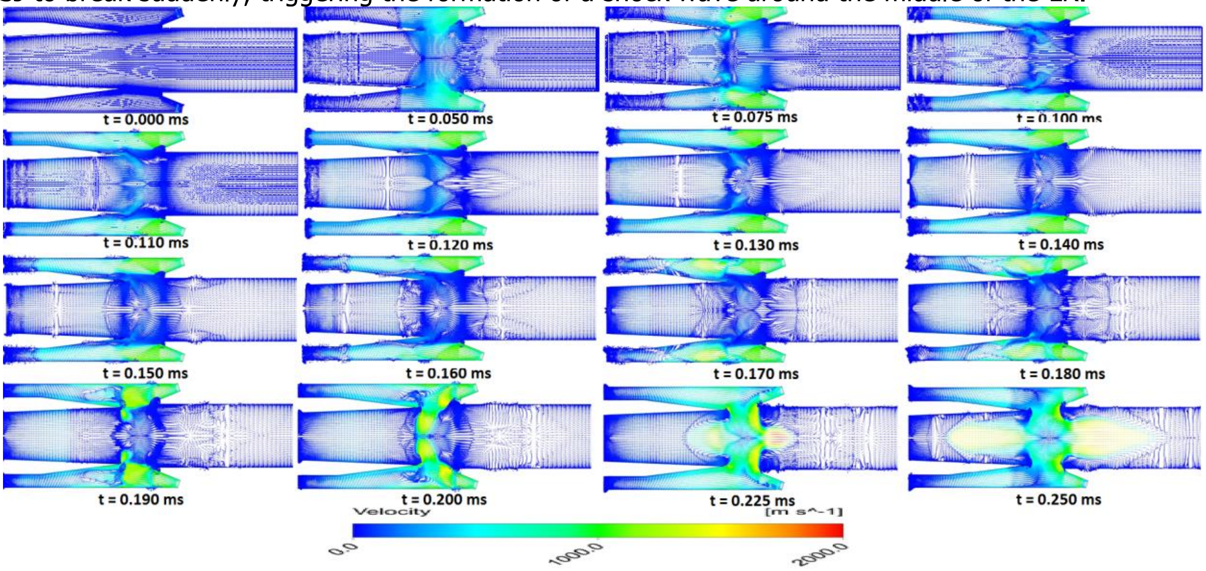

Figure 3 – Velocity vector field evolution during the ignition phase

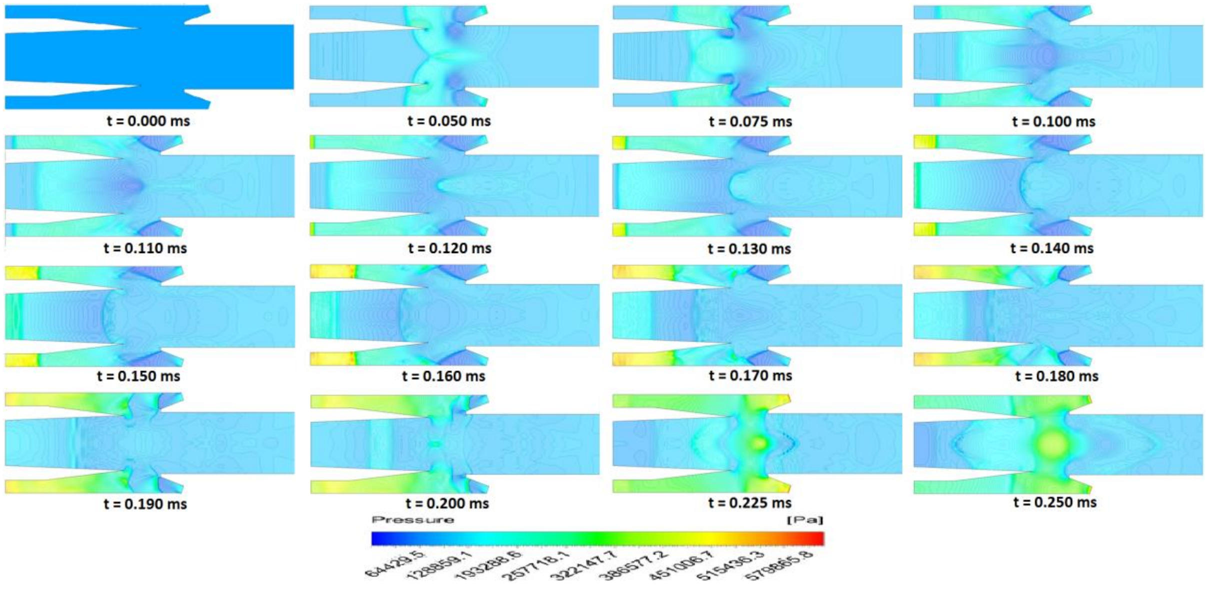

Figure 4 – Pressure scalar field evolution during the ignition phase

At this point, the temperature rises sharply through the shock wave (Fig. 2) due to the meeting of the two suddenly breaking air streams, and the fuel – air mixture starts propagating upstream, as a deflagration wave, through the fresh mixture in the SJ. A secondary couple of ignition points appears on the LR walls at t = 160 ms, possibly due to wall friction (Figs. 2 and 6), helping to propagate the combustion wave into the fresh mixture. However, these secondary ignition points may be an artifact of the numerical simulation, due to an insufficient resolution of the computational grid. The limited available computational power prevented the use of a higher resolution grid to further test the issue. In any case, the two combustion region merge at t = 0.170 ms, reducing the importance of the secondary ignition points, since they are enveloped in the burned region in any case.

The combustion process spreads through the LR, which are almost completely filled with combustion products at t = 0.180 ms. It is important to note that regions near the LR closed ends remain untouched by the combustion process, as the combustible mixture was never convected by the incoming SJ jets this region in the initial stages of the process. This may be one of the optimization issues to be solved in the future, but the complete elimination of this region may prove impossible, since a volume of increasingly higher pressure must exist at the LR closed ends.

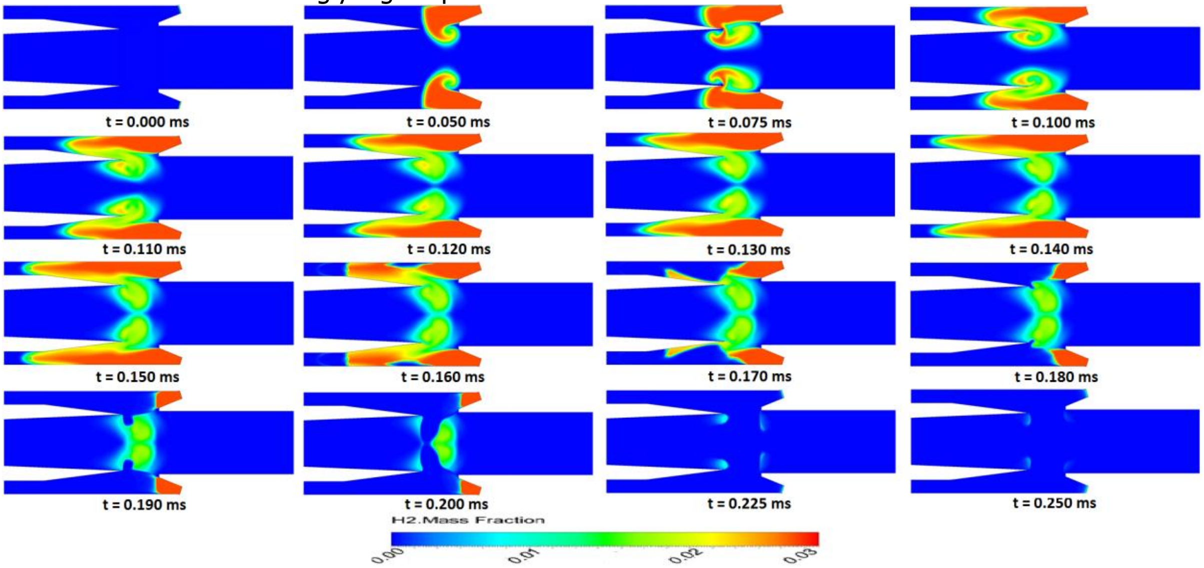

Figure 5 – Hydrogen mass fraction scalar field evolution during the ignition phase

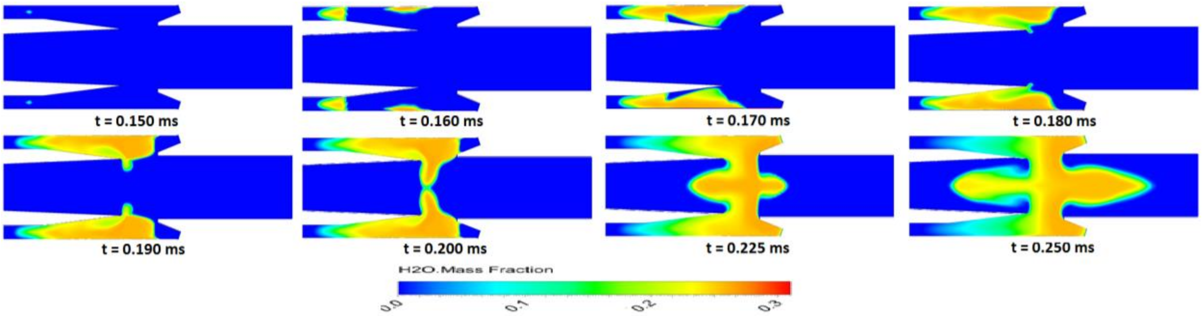

Figure 6 – Water mass fraction scalar field evolution during the ignition phase

Meanwhile, this shock wave propagates upstream through the LR increasing the local pressure. Typical shock cell structures can be observed in Fig. 4 at t = 0.180 ms. While the SN flow is still under-expanded, it tends to further expand downstream of the SN through an expansion fan [32]. These expansion waves reflect on both the fluid boundary of the jet, and on the solid surface of the wall, but the effect of the reflection is different in the two cases. On the fluid surface, constant pressure at the boundary must be preserved, therefore the reflection on the fluid boundary creates shock waves returning into the jet. On the contrary, to ensure the no-slip wall condition, the waves reflected back into the jet remain expansion waves. Thus, these alternating expansion and compression regions create a stationary structure of so-called shock cells [33]. Similar behavior of SJ in the close neighborhood of solid walls is frequently reported in the literature (e.g. [33]).

The increasing pressure starts flattening the bow expansion wave formed at the exhaust of the two SN, while also pushing it back, inside the SN, staring at t = 0.190 ms (Fig. 4).

The local pressure in the LR regions close to the outer walls increases, and the direction of the incoming SJ is deflected towards the central region of the PDC (Fig. 3). The flow in the LR reverses direction and is directed now towards the SN. At this time (t = 0.190 ms), the flame reaches the central region of the PDC (Figs. 2 and 6), and starts propagating mainly transversally through the combustible mixture brought here by the entrainment vortices mentioned earlier, at t = 0.200 ms (Fig. 5). The sudden increase in temperature in the CDC inlet triggers a sudden increase in pressure in the central region of the PDC at t = 225 ms (Fig. 4). The pressure gradient occurring between this region and the neighbouring zones, both upstream and downstream, creates a strong axial acceleration, up to supersonic values (Fig. 3). The incoming SJ suffer a sharp turn immediately after exiting the SN, and the flow pattern at t = 0.250 ms becomes similar to the non – reactive case flow

[34] (Fig. 3). A central SJ jet oriented towards the PDC outlet is formed, delimited by a strong shock wave also propagating outwards (Fig. 4). The combustion front is coupled and rides right behind this travelling shock wave, in a typical detonation front pattern (Figs. 2 and 6). The pressure in the SN is higher now than the inlet pressure (Fig. 4), and the flow of fresh mixture into the PDC is blocked.

In the CDC, pressure waves are propagating from the central region towards the closed end starting with the inception of the flow, driven tangentially by the incoming SJ. These waves travel slower in the CDC than in the LR, due to the larger volume available in the central region. The initial pressure wave reaches the back wall of the CDC only at t = 0.140 ms, and the pressure in the pocket created between the reflected pressure wave and the back wall is much lower than in the similar pockets created in the LR. The combustible mixture does not have sufficient time to reach the CDC (Fig. 5), so no ignition occurs here. Once the detonation wave is created in the central PDC region, the strong pressure gradient it creates also propagates into the CDC and overcomes the reflected pressure wave, driving a high speed flow towards the back wall. The CDC plays no active role in this phase.

3.2 The detonation propagation phase: 0.250 - 0.600 ms

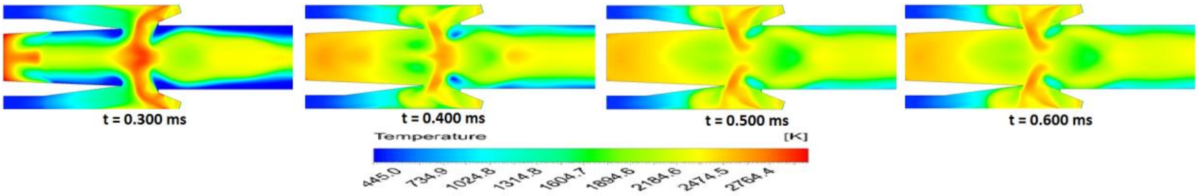

Figure 7 – Temperature scalar field evolution during the detonation propagation phase

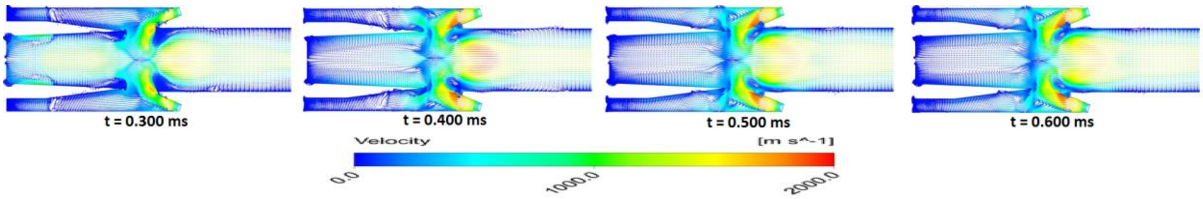

Figure 8 – Velocity vector field evolution during the detonation propagation phase

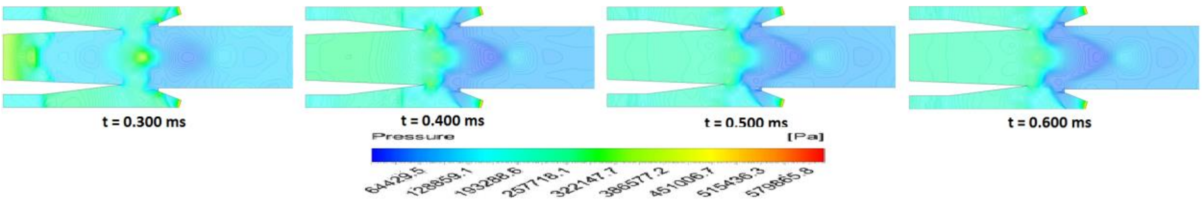

Figure 9 – Pressure scalar field evolution during the detonation propagation phase

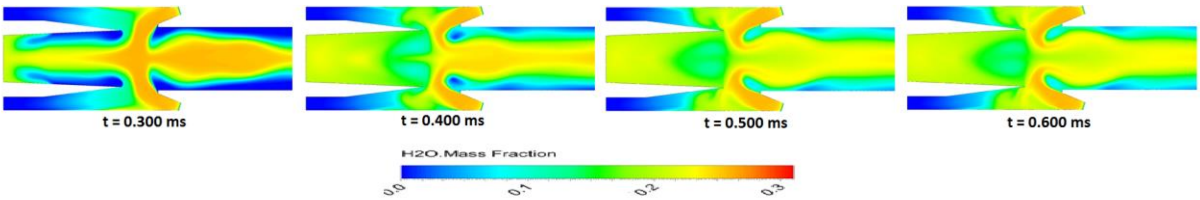

Figure 10 – Water mass fraction scalar field evolution during the detonation propagation phase

Once the detonation is initiated in the central region around t = 0.225, the detonation wave starts propagating towards the PDC exit. Figs. 7 – 10 present the evolution of, respectively, temperature, velocity vector, pressure, and water mass fraction between 0.300 ms and 0.600 ms. The Hydrogen mass fraction field is omitted, as the Hydrogen amounts in the PDC in this phase are negligible.

The velocity in the central jet core increases up to t = 0.400 ms (Fig. 8), as long as it is supported by combustion (Figs. 7 and 10). The acceleration is mainly axial (Fig. 8). The direction of the SJ remains largely unchanged (Fig. 8), with a sharp turning of the jets immediately downstream of the SN exits, due to the large pressure in the region between the SN exits and the entrance in the LRs (Fig. 9).

In the central jet region, the pressure gradually decreases as the combustion process stops due to fuel depletion. The pressure wave propagating towards the CDC back wall reaches it between t = 0.300 ms and t = 0.400 ms and is reflected back, while the pressure behind decreases due to the

increasing available volume. Due to the combined effect of disappearing combustion and expansion behind the reflected wave, the pressure in the CDC tends towards a uniform value at t = 0.500 ms.
No significant amounts of Hydrogen were observed in the computational domain in this phase. In the LR and at the exit of the two SN, the pressure levels remain high enough to stop the admission of the fresh mixture into the PDC. However, the temperature inside the SN remains high enough (Fig. 7) to continue to ignite the fresh mixture whenever the pressure in the divergent section of the SN decreases enough to allow it to enter the computational domain. This situation can be observed at t = 0.600 ms, when the pressure in the SN tends to drop (Fig. 9), due to the entrainment effect created by the high speed turning jets (Fig. 8). However, the ignition of the fresh mixture immediately as it enters the PDC raises back the pressure and stops again the admission.
This effect is an artefact of the numerical simulation, in contradiction with the experimental observations [35]. Several reasons may be responsible for the numerical simulation not capturing the actual behavior of the flow inside the PDC. First, the used combustion model (EDM) is known to overpredict the flame thickness in reactive flow simulations [36]. As a result, the flame is less responsive to flow gradients, particular velocity gradients creating stresses and strains, and is much harder to quench [37]. Also, the boundary condition imposed on the PDC solid walls were specific to adiabatic walls, preventing the normal loss of heat through the wall to the environment and artificially supporting a high temperature. Finally, the computational domain is limited to the critical section of the SN, thus preventing pressure waves to travel upstream into the subsonic region of the SN, and to create full flow reversal through the SN. This way, the fresh mixture is always ready to enter the diverging part of the SN supporting combustion and not allowing the proper cooling of the flow inside the SN. To circumvent this shortcoming of the numerical simulation, the flow through the two SN was artificially stopped by closing the computational domain inlets placed in the critical sections of the SN.

3.3 The flow cooling phase: 0.600 - 0.900 ms

As mentioned before, the numerical simulation in this phase used a zero velocity boundary condition at the inlet. The results are presented in Figs. 11 – 13, showing, respectively, the scalar temperature field, the velocity vector field, and the scalar fields of pressure and water mass fractions. Figures also include the fields at 1.0 ms, in the readmission phase. Since the admission of fresh mixture in the computational domain is blocked, the Hydrogen mass fraction field is omitted. Also, the water mass fraction field closely follows the temperature field, and is omitted as well.

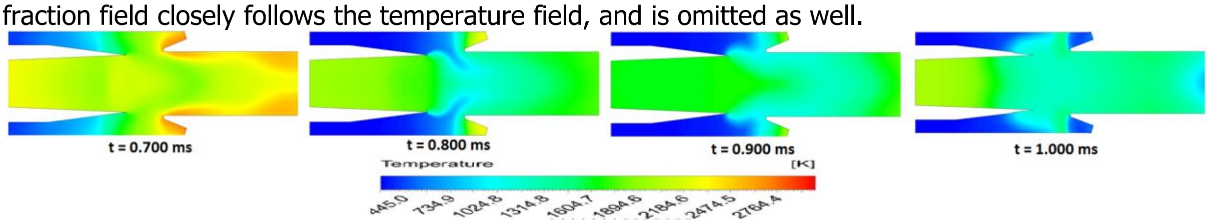

Figure 11 – Temperature scalar field evolution during the flow cooling phase

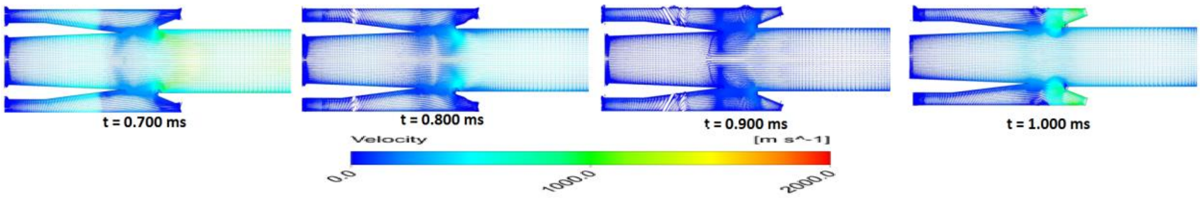

Figure 12 – Velocity vector field evolution during the flow cooling phase

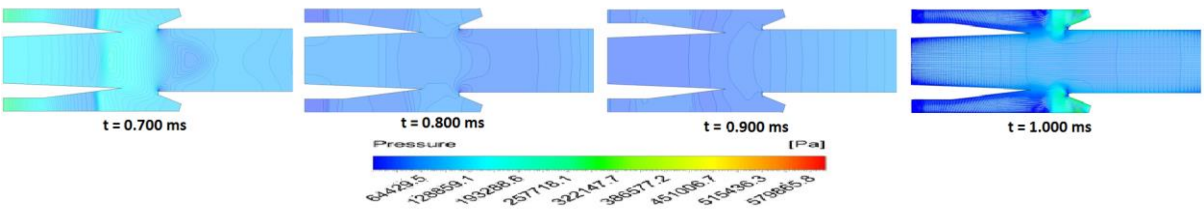

Figure 13 – Pressure scalar field evolution during the flow cooling phase

The effect of closing the inlet SN is immediately visible in the velocity field. The tangential velocity decreases suddenly (Fig. 12) once the incoming SJ disappear, and remain at very low values throughout the current phase. The axial velocity approaches zero almost immediately after the inlets

are closed, at t = 0.700 ms (Fig. 12). The central jet velocity decreases much slower, supersonic velocities being maintained up to 0.800 ms. The CDC velocity also decreases, at about the same pace. As the jets disappear, the flow angle in the central region decreases gradually (Fig. 12), the influence of the removed SJ being still felt at t = 0.900 ms, albeit weakly.
The temperature starts also decreasing throughout the PDC (Fig. 11), with high temperature regions being maintained towards the outlet, where the influence of the hot central jet core is still present, and near the walls, particularly in the CDC and in the divergent parts of the two SN. The LR cool much faster, since their temperature was much lower at the beginning of the phase anyway.
The water mass fraction field evolves in a pattern very similar to the temperature. Since, in the absence of combustion, no more water is produced, the water accumulated in the CDC and, partially, in the divergent section of the two SN is convected away, towards the exhaust of the PDC. It is noteworthy that the central detonation region remains filled by combustion products even at t = 0.900 ms. It is, therefore, very unlikely that this region will be washed during the next detonation cycle, and the combustion products replaced by fresh mixture. Hence, the participation of the CDC in the actual detonation process is reduced in this PDC design. This will have to be addressed, and the shape and size of the CDC represents an obvious target for further optimization studies. One possible approach is to increase the angle of the SJ to direct a larger part of the fresh mixture into the CDC.
The pressure starts decreasing first in the middle of the region between the central jet core and the back wall, both in the CDC and in the LR, as seen at t = 0.700 ms (Fig. 13). The pressure waves are reaching the back wall and are reflected back towards the outlet (t = 0.800 ms), while the general pressure level inside the PDC continues to decrease towards the atmospheric level, at t = 0.900 ms.

3.4 The flow cooling phase: 0.900 - 1.000 ms

Once the temperature downstream of the critical sections of the two SN dropped below the self – ignition point for Hydrogen, the initial simulation boundary conditions were reinstated, allowing fresh mixture to be admitted. The results are presented in the rightmost position in Figs. 11 – 13.
Obviously, fresh mixture enters the divergent region of the two SN and is convected into the PDC. The colder fresh mixture decreases the temperature in the SN below the ignition point of the fuel (Fig. 11), and no combustion products are formed in the SN. The pressure rises into the SN again (Fig. 13), and creates pressure waves that start propagating mainly into the two LR, restarting the detonation cycle. As before, the direction of the SJ exiting the SN is towards the LR (Fig. 12). From this point, the flow patterns inside the PDC are repeating the previous cycle, with a new ignition phase, followed by the detonation propagation phase, and the cooling phase.

4 FUTURE DEVELOPMENT DIRECTIONS

The numerical simulation of pulsed detonation flows is one of the most challenging problems in CFD and the results currently presented in the literature have only met with limited success (e.g. [38]. Significant numerical issues have been also encountered during the study presented herein. The reasons for the shortcomings are numerous, and they are directly resulting from the complex physics underlying the detonation process. To achieve reasonable accuracy, the intricate structure of the detonation wave needs to be captured. Generally, e.g. [39], a detonation wave is described as a shock wave that performs an adiabatic compression of the fuel mixture gas, followed by a thermally neutral induction zone, where the temperature and pressure remain close to their post-shock values while the reactants undergo chain initiation reactions producing free radicals. When a sufficient amount of free radicals is produced, a reaction zone develops downstream of the initiation zone, and the temperature increases substantially, due to the effect of highly exothermal chain branching reactions. The pressure decreases via expansion waves that create a forward thrust that supports the shock front. The discretization grid employed by the simulation must be fine enough to capture this wave, down to microns resolution [40], close to a Direct Numerical Simulation (DNS) size grid.
The resolution of the numerical grid employed in this study was harshly limited by the available computational resources, even though it is below 350 η. The results show that this was not sufficient to accurately represent the near wall regions under the very high velocity conditions typical for detonation, possibly leading to the secondary ignition points in Fig. 2. A Large Eddy Simulation (LES) of the flow is necessary, and is planned for the near future.
Furthermore, the complexity of the chemical reaction mechanism used to model the Hydrogen oxidation needs to be sufficient to include realistic chemical reaction steps able to capture the key

dynamics of pulsed detonation [41]. Complex mechanisms for Hydrogen combustion are available, but the computational workload resulting from applying a them on a near-DNS computational grid renders the simulation almost unfeasible due to the huge computational resources required. To alleviate this, a combustion model able to model the effects of finite rate multi-step combustion at a sub-grid level, and thus permitting the use of a lower resolution needs to be developed.

5 CONCLUSIONS

The reactive numerical simulations presented in the paper confirm the self – ignition of the fuel inside the PDC and capture very well the ignition phase of the detonation process. The SJ entering the PDC through the two SN are first directed towards the two LR, where they trigger pressure waves that propagate towards the closed ends of the resonators, where they are reflected back towards the SN. When the reflected pressure waves meet the incoming jets, a couple of shock waves is formed. The temperature rise through these shock waves raises the temperature above the self – ignition point of Hydrogen and initiates combustion inside the PDC. The combustion wave propagates, as deflagration, through the LR and escapes into the central region of the PDC, igniting the fresh mixture convected here by jet entrainment created eddies. In the mean time, the pressure increases in the LR due to combustion, and the high pressure zone approaches the SN, forcing the two SJ to detach from the wall and turn towards the central region of the demonstrator, forming a central SJ core delimited by a shock wave. Here, the combustion wave accelerates and turns into a detonation wave formed by the coupling of the combustion wave with the shock wave delimiting the central jet core. The detonation wave subsequently propagates towards the PDC outlet. The numerical simulation fails to properly capture the next phase of the cycle due to combustion model limitations and wall boundary conditions issues. To simulate the cooling phase, the two inlets were artificially closed until the temperature immediately downstream of the two SJ dropped below the self – ignition value. After this, the initial boundary conditions were reinstated, and a new detonation cycle begun. Possible approaches to address the issue are presented. In the current design, the CDC does not play a significant role in the operation of the PDC, as it remains filled with burned products at the end of the detonation cycle and is never fully filled with fresh mixture. Further design optimization is required in the future.

ACKNOWLEDGEMENT

This work was funded by the European Commission, through the Framework Programme 7 European research project no. 335091 – TIDE

REFERENCES

1. D.L. Chapman, 1889. "On the Rate of Explosion in Gases," *Ph. Mag. S. 5*, **47** (284), pp. 90–104
2. E. Jouguet., 1905, "Sur la propagation des reactions chimiques dans les gaz", *Journal des Mathematiques Pures et Appliquees*, **1**, pp. 347–425
3. Y.B. Zeldovich, 1940, "K Teoriras prostranenia detonazi v gasoobrasnikh systemakh", *Zhurnal Experimentalnoii Teoreticheskoi Fiziki*, **10**, pp. 543–568
4. J. von Neumann, 1963, "Theory of Detonation Waves", Progress Report to the National Defense Research Committee, Div. B, OSRD-549, (April 1, 1942. PB 31090), Ed. A. H. Taub in "*John von Neumann: Collected Works, 1903–1957*", **6**, Pergamon, New York
5. W.H. Heiser, D.T. Pratt, 2002, "Thermodynamic Cycle Analysis of Pulse Detonation Engine", *Journal of Propulsion and Power*, **18** (1), pp. 68–76
6. R. Bellini, F.K. Lu, 2010, "Exergy analysis of a pulse detonation power device", *Journal of Propulsion and Power*, **26** (4), pp. 875–878
7. K. Kailasanath, 2000, "Review of Propulsion Applications of Detonation Waves", *AIAA J.*, **38** (9)
8. N. Hoffmann, 1940, "*Reaction Propulsion by Intermittent Detonative Combustion*", German Ministry of Supply, AI152365, Volkenrode Translation, 1940
9. N. Shachtman, 2008, "*Explosive Engines Key to Hypersonic Plane*", Conde Nast Publications, San Francisco, CA, U.S.A
10. L.H. Back, W.L. Dowler, G. Varsi, 1983, "Detonation Propulsion Experiments and Theory", *AIAA Journal*, **21** (10), pp. 1418–1427
11. G.P. Menees, H.G. Adelman, J.L. Cambier, J.V. Bowles, 1992, "Wave Combustors for Trans-Atmospheric Vehicles", *Journal of Propulsion and Power*, **8**(3), pp. 709–713

12. L.H. Back, W.L. Dowler, G. Varsi, 1983, "Detonation Propulsion Experiments and Theory", *AIAA Journal*, **21** (10), pp. 1418–1427
13. L.H. Back, 1975, "Appl. of Blast Wave Theory to Explosive Propulsion", *A. Astr.*, **2**, pp. 391–407
14. R.J. Pegg, B.D. Couch, L.G. Hunter, 1996, "Pulse detonation engine air induction system analysis" *AIAA Paper 96-2918*, AIAA Meeting Papers on Disc
15. A.J. Dean, K.R. McManus, V.E. Tangirala, 2006, "*Multiple detonation initiator for frequency multiplied pulsed detonation combustion*", US Patent US7131260
16. S.Y. Lee, J. Watts, S. Saretto, S. Pal, C. Conrad, R. Woodward, R. Santoro, 2004, "Deflagration to Detonation Transition Processes by Turbulence-Generating Obstacles in Pulse Detonation Engines", *Journal of Propulsion and Power*, **20** (6)
17. N. Smirnov, 2007, "Pulse Detonation Engines: Advantages and Limitations", in "*Advanced Combustion and Aerothermal Technologies, NATO Science for Peace and Security*", Series C: Environmental Security, **6**, pp. 353-363
18. F. Ma, J.Y. Choi, V. Yang, 2008, "Internal Flow Dynamics in a Valveless Airbreathing Pulse Detonation Engine", *Journal of Propulsion and Power*, **24** (3)
19. V.L. Reingold, A. Quillevere, G. Delange, 1952, "Perfectionnements apportés aux foyers à circulation interne supersonique, notamment aux chambres de combustion pour moteurs à réaction d'aérodynes", French Patent FR1008660
20. V.M. Shmelev, S.M. Frolov, 2010, "Method and Device for Developing Thrust", Pat. RU2179254
21. J.H.S. Lee, 1984, "Dynamic param. of gas detonations", *Ann. Rev. Fl. Mech.*, **16**, pp. 311- 336
22. I.M. Bychkov, V.V. Vyshinsky, L.V. Nosachev, 2009, "Investigation of the flow pattern in a gas-jet Hartmann resonator", *Technical Physics*, **54** (8), pp. 1110-1115
23. M. Brouillette, J.S. Plante, 2008, "Rotary Ramjet Engine", US Patent US7337606
24. B.G. Kramer, 1918, "Rotary Explosion Engine" US Patent US1287049
25. G.D. Roy, S.M. Frolov, A.A. Borisov, D.W. Netzer, 2004, "Pulse Detonation Propulsion: Challenges, Current Status, and Future Perspective," *Prog. Enrg. Comb. Sci.*, **30** (6), pp. 545–672
26. C.F. Cuciumita, B.G. Gherman, I. Porumbel, 2013, "Novel Pulse Detonation Engine Concept", *CEAS 2013 Air and Space Conference – Innovative Europe*, Linkoping, Sweden
27. T. Cuciuc, C.E. Hritcu, G.G. Ursescu, I. Porumbel, C.F. Cuciumita, 2017, "Valveless Pulsed Detonation Chamber Controlled by Hartmann Oscillators ", *CEAS 2017*, 16 - 20 Oct., Buch., Romania
28. B.F. Magnussen, B.H. Hjertager, 1976, "On mathematical models of turbulent combustion with special emphasis on soot formation and combustion", *16th Symp. (Intl.) Comb.*, Combustion Institute
29. A. Tyliszczak, A. Boguslawski, D. Nowak, 2016, "Numerical simulations of combustion process in a gas turbine with a single and multi-point fuel injection system "; *Applied Energy*, **174**, pp. 153-165
30. N.M. Marinov, C.K. Westborrk, W.J. Pitz, 1996, "Detailed and Global Chemical Kinetic Model for Hydrogen", *Transport Phenomena in Combustion*, **1,** Taylor and Francis
31. S.B. Pope, 2000, "*Turbulent Flows*", Cambridge University Press,
32. J.D. Anderson, 1990, "*Modern Compressible Flows*", McGraw-Hill, Second Edition
33. C. Lubert, 2009, "The Primary Noise Sources Associated with Turbulent Coanda Wall Jets", *The 16th International Congress on Sound and Vibration*, Krakow, 5 – 9 July
34. I. Porumbel, T. Cuciuc, C.F. Cuciumita, C.E. Hritcu, F.G. Florean, 2014, "Large Eddy Simulation of Non-Reactive Flow in a Pulse Detonation Chamber", *Advances in Applied and Pure Mathematics. Proc. 7th Intl. Conf. Finite Diff., Finite Elem., Finite Vol., Bound. Elem. (F-and-B '14)*, Gdansk, Poland
35. I. Porumbel, C.F. Cuciumita, C. Nechifor, R. Kuncser, T. Cuciuc, 2017, "Experimental Measurements in Hartmann Oscillators", *CEAS 2017*, 16 - 20 Oct., Bucharest, Romania
36. I. Porumbel, 2006, "Large Eddy Simulation of bluff body stabilized premixed and partially premixed combustion", *Ph.D. Thesis,* Georgia Institute of Technology, Atlanta, Georgia, USA
37. I. Porumbel, 2007, "Effect of inflow equivalence ratio variation on bluff body stabilized premixed flames", *Thermal Engines and Environmental Engineering METIME 2007*, Galaţi, Romania
38. F.J.S. Velasco, R.A. Oton-Martinez, J.R. Garcıa-Cascales, S. Espın, N. Meynet, A. Bentaib, 2016, "Modelling detonation of H2-O2-N2 mixtures in presence of solid particles in 3D scenarios", *International Journal of Hydrogen Energy*, **41**, pp. 17154 - 17168
39. W. Fickett, W.C. Davis, 1979, "*Detonation*", University of California Press
40. N. Tsuboi, 2007, "Numerical approach on hydrogen detonation: fundamentals and applications", *2nd European summer school on hydrogen safety*, Belfast, UK
41. M. Short, J.J. Quirk, 1997, "On the nonlinear stability and detonability limit of a detonation wave for a model three-step chain-branching reaction", *Journal of Fluid Mechanics*, **339**, pp. 89 - 119